Technical Paper

Analytical Evaluation of the Surface Integral in the Singularity Methods

By

Suh, Jung-Chun*

특이점분포법의 표면적분항의 해석적 계산

서정천*

Abstract

For a planar curve-sided panel with constant or linear density distributions of source or doublet in the singularity methods, Cantaloube and Rehbach (1986) show that the surface integral can be transformed into contour integral by using Stokes' formulas. As an extension of their formulations, this paper deals with a planar polygonal panel for which we derive the closed-forms of the potentials and the velocities induced by the singularity distributions.

Test calculations show that the analytical evaluation of the closed-forms is superior to numerical integration (suggested by Cantaloube and Rehbach) of the contour integral. The compact and explicit expressions may produce accurate values of matrix elements of simultaneous linear equations in the singularity methods with much reduced computer tiome.

요   약

평면판 요소에 균일한 혹은 선형적인 세기를 갖는 쏘오스 또는 다이폴이 분포된 경우, Stokes 정리를 이용하여, 표면 특이점 분포방법에서 나타나는 표면 적분식을 선적분 형태로 변환할 수 있다. 더우기 판 요소가 다각형인 경우, 유기 포텐시얼과 유기속도를 구하기 위한 이 선적분의 closed-forms을 유도하였다. 이들 적분식의 해석적 계산을 통해 계산시간을 단축하고 수치해의 정도를 향상시킬 수 있을 것이다. 몇개의 계산예를 통해 해석적 적분 계산이 수치적 적분보다 우수함을 알 수 있다.

1. Introduction

The fundamental problem for computing the potential flow about arbitrary bodies is to determine velocity potential ϕ in a simply connected fluid domain. Using Green's scalar identity, the velocity potential can be represented from distributions of sources and doublets on the boundary surfaces. Applying the normal boundary condition (that is, the no-penetration condition) at the collocation points in the potential-based panel methds (which have been widely used in marine hydrodynamics) results in a linear system of algebraic equations to be soved for unknown doublet strengths on each panel (or at each vertex) with known source strengths. The associated surface integrals should be evaluted at the collocation points to obtain the matrix elements of the linear system. Therefore a fast and accurate computation of these elements is very important in the numerical solution.

In the singularity methods to the potential flow problem, the potential ϕ within the fluid domain D can be expressed approximately as a sum of each contribution in terms of the surface value of ϕ and its normal derivativ $n \cdot \nabla \phi$ on each panel of the discretized boundary surfaces S_i;

$$\phi(x_p) = -\frac{1}{4\pi}\sum_i \iint_{S_i} \{\frac{1}{r}n \cdot \nabla_\zeta\phi - \phi\, n \cdot \nabla_\zeta (\frac{1}{r})\}\, dS_\zeta \tag{1}$$

Here the subscript ζ refers to an integration variable. r is a distance between an integration point x_ζ on S_i and any field point x_p located in D. The first and the second term in the integral represent the potential due to a surface distribution, respectively, of source-type singularity with a density $\sigma \equiv n \cdot \nabla \phi$ and of doublet-type singularity with a density $\mu \equiv -\phi$. The velocity components can be derived by differentiation of Eq. (1) with respect

to the coordinates of the field point. We may take without loss of generality one planar panel as the integration region concerned herein, which can be regarded as a part of the discretized boundary surface.

The closed-form expressions of the surfce integrals for constant source distributions over flat quadrilateral panels have been introduced by Hess & Smith (1966). They expressed the surface integrals as a superposition of line integrals for each side of the panels, with independent treatment of the contribution from the side. Webster (1975) has extended the Hess and Smith analysis to a triangular panel in order to eliminate the discontinuity problem for a flat quadrilateral source panel by allowing a linear variation of the source strength across the triangular panel. These two approaches are concerned with only the source distributions and the resultant expressions are considerably complicated to employ a computer code. A simpler and more unified derivation has been provided by Newman (1986) for computing the potential due to a constant doublet or source distribution. His analyses are based on the elementary plane geometry related to the solid angle of a panel. He defined four infinite sectors (for a quadrilateral panel), bounded by semi-infinite extensions of the two adjacent sides of the panel with respect to the corresponding vertices, such that the difference between the domains of the four sectors is the domain of the panel. Then the surface integral over each infinite sector is evaluated in terms of the included angle of the corresponding vertex projected onto the unit sphere with center at the field point. He has also described the more general recursive scheme for computing the potential due to a source or doublet distribution of linear, bilinear or higher order form. However the corresponding results for the induced velocities due to such singularity distributions do not appear explicitly.

Another elegant approach based on mathematical formulations has been presented by Cantaloube & Rehbach (1986), by which they introduced more explicit expressions of the surface integrals for the source or doublet distribution. With vector operations of the integrands for using Stokes' formulas, they show that the surface integrals for the constant or linear distributions of sources and doublets over a planar facet can be transformed into line integrals along the contour of the panel. First, for subsequent use in the following sections, we take here their resultant expressions for the induced potentials ϕ and the induced velocities V : for a source distribution,

$$\phi^{(\sigma)} = -\frac{1}{4\pi}\left[\underline{n}\cdot\oint_C \sigma\frac{\underline{r}}{r}\times d\underline{l}_\xi - (\underline{n}\cdot\underline{r})\oint_C \sigma A\cdot d\underline{l}_\xi \right. $$
$$ + (\underline{n}\cdot\underline{r})(\underline{n}\cdot\underline{e})\underline{n}\cdot\{\nabla\sigma\times\oint_C \ln(r+\underline{e}\cdot\underline{r})\,d\underline{l}_\xi\} $$
$$ \left. -\underline{n}\cdot(\nabla\sigma\times\oint_C r d\underline{l}_\xi)\right] \qquad (2)$$

$$V^{(\sigma)} = -\frac{1}{4\pi}\left[\underline{n}\cdot\oint_C \sigma A\cdot d\underline{l}_\xi + \underline{n}\times\oint_C \frac{\sigma}{r}\,d\underline{l}_\xi \right. $$
$$ -\underline{n}(\underline{n}\cdot\underline{e})(\underline{n}\times\nabla\sigma)\cdot\oint_C \ln(r+\underline{e}\cdot\underline{r})\,d\underline{l}_\xi $$
$$ \left. +\nabla\sigma\{\underline{n}\cdot\oint \frac{\underline{r}\times d\underline{l}_\xi}{r} - (\underline{n}\cdot\underline{r})\oint_C A\cdot d\underline{l}_\xi\}\right] \qquad (3)$$

and for a doublet distribution,

$$\phi^{(\mu)} = -\frac{1}{4\pi}\{-\oint_C \mu A\cdot d\underline{l}_\xi + (\underline{n}\cdot\underline{e})(\underline{n}\times\nabla\mu)\cdot $$
$$ \oint_C \ln(r+\underline{e}\cdot\underline{r})\,d\underline{l}_\xi\} \qquad (4)$$

$$V^{(\mu)} = -\frac{1}{4\pi}\{\oint_C \mu\nabla_\xi(\frac{1}{r})\times d\underline{l}_\xi - \nabla\mu\oint_C A\cdot d\underline{l}_\xi $$
$$ - (\underline{n}\times\nabla\mu)\times(\underline{n}\times\oint_C \frac{d\underline{l}_\xi}{r})\} \qquad (5)$$

It is noted that the signs of the third and the fifth integral in Eq. (3) and the second and the third intregral in Eq. (5) are opposite to those in the original paper (see Suh (1990a)). The superscripts (σ) and (μ) refer to the source and the doublet

singularity respectively. The contour integrals are performed along the perimeter of the panel C in a counterclokwise sense. The unit normal to the surface $\underline{n}$ points outward in the sense of a right-handed-rule and $d\underline{l}_\xi$ is the integration element along the contour C. The distance vector $\underline{r}$ is defined as $\underline{x}_\xi - \underline{x}_p$ where the subscripts ξ and p refer to the source point and the field point respectively. The unit vector $\underline{e}$ is taken as $\pm\underline{n}$ where the sign is chosen such that $\underline{e}\cdot\underline{r}$ is not negative. For the use of Stokes' formulas they used the following key relation introduced by Guiraud (1978) :

$$\nabla(\frac{1}{r}) = -\nabla\times\underline{A}, \text{ with } \underline{A} = \frac{\underline{e}\times\underline{r}}{r(r+\underline{e}\cdot\underline{r})} \qquad (6)$$

Here Eq. (6) holds for more generally $\underline{e}$ independent of the integration point $\underline{x}_\xi$.

The major advantages of their study are that the formulations are valid for a planar curve-sided panel and that the resultant equations are expressed in a global coordinate wystem while the aforementioned analyses require the transformation of the local coordinate system. Thus the expressions derived by Cantaloube & Rehbach may be regarded as a more computer-oriented from. They have proposed the use of direct numerical integrations of the line integrals by an integration quarature (e.g. Simpson rule or Gaussian quadrature), illustrating the numerical consistency and accuracy for a linear doublet distribution on a quadrilateral panel. However when a field point is very close to the sides or vertices of a panel, a large number of the quadrature base points and considerable effort to choose these points suitably would be needed in order to achieve good comparisons with the known values. Such numerical implementation in a computer code may lead to a large amount of extra-computer time.

As an extension of the formulation of Cantaloube & Rehbach, the present paper deals with a

planar polygonal panel (i.e. with a planar panel with an arbitrary number of sides) for which the line integrals given in Eqs. (2) through (5) can be reduced to the closed-forms. Derivation of these closed-forms is the main scope of the present paper. The closed-form expressions for the potential and velocity induced by a constant source distribution are presented in section 2. They are expressed compactly as a sum of contribution from each side of the panel, in terms of appropriate basic integrals. It will be shown that each contribution depends on the relative position of a field point with respect to the side. Also we will consider the limiting cases that the field point approaches directly above or below the panel surface (the self-induction cases) in order to ensure the required singular behavior of the potential and the velocity. The corresponding results for a doublet distribution of constant strength are provided in section 3. Section 4 is devoted to analytical evaluations of the basic integrals derived in the preceding sections. In section 5, a similar approach is developed to extend the anayses to a linear variation of soure or doublet strength, which provides continuous singularity strength distributions on triangular panels. In section 6, for the purpose of checking the convenience and accuracy of the present approach, we take constant distributions of singularities on a rectangular panel of a large aspect ratio and some field points in the extreme vicinity of the panel. Test computations of the associated line integrals at the field points show an advantage of the analytical evaluations over numerical integrations recommended by Cantaloube & Rehbach. The same aspect appears in comparisons of the potentials and velocities.

2. Constant Source Distribution

The potential at any field point $\underline{x}$, (x, y, z) induced

by a distribution of sources with unit density $\sigma = 1$ can be written as, by taking the first two integrals from Eq. (2),

$$\phi^{(a)} = -\frac{1}{4\pi}\{\underline{n}\cdot\oint_c \frac{\underline{r}}{r}\times d\underline{l}_{\underline{\iota}} - (\underline{n}\cdot\underline{r})\oint_c \underline{A}\cdot d\underline{l}_{\underline{\iota}}\} \quad (7)$$

Using Eq. (6) for $\underline{A}$, we can write

$$\phi^{(a)} = -\frac{1}{4\pi}\{\underline{n}\cdot\oint_c \frac{\underline{r}}{r}\times d\underline{l}_{\underline{\iota}} - (\underline{n}\cdot\underline{r})\cdot$$

$$\oint_c (\frac{1}{r} - \frac{1}{r+\underline{e}\cdot\underline{r}})\frac{\underline{e}\times\underline{r}}{\underline{e}\cdot\underline{r}}\cdot d\underline{l}_{\underline{\iota}}\}$$

$$= -\frac{1}{4\pi}\oint_c \frac{\underline{r}\cdot(d\underline{l}_{\underline{\iota}}\times n)}{r+\underline{e}\cdot\underline{r}} \quad (8)$$

Note that find the following useful relation from this rearrangement :

$$\frac{1}{r} = \underline{e}\cdot\nabla\times\underline{B}, \quad \text{with } \underline{B} = \frac{\underline{e}\times\underline{r}}{r+\underline{e}\cdot\underline{r}} \quad (9)$$

The term $\underline{r}\cdot(d\underline{l}_{\underline{\iota}}\times n)/d\underline{l}_{\underline{\iota}}$ represents the projection of the distance vector $\underline{r}$ onto the vector perpendicular to both $d\underline{l}_{\underline{\iota}}$ and $\underline{n}$. Because it is constant for each side of a straightline and $\underline{e}\cdot\underline{r}$ (that is, the normal distance of the field point from the panel) is constant for a planar panel, Eq. (8) can be written as

$$\phi^{(a)} = -\frac{1}{4\pi}\sum_{i=1}^{N_s} b_i \int_{c_i} \frac{1}{r+a}dl_{\underline{\iota}} \quad (10)$$

where N_s is the number of sides of the polygon panel (for example, $N_s = 3$ for triangular panels), $a = \underline{e}\cdot\underline{r}$ is a non-negative constant value for all sides, and $b_i = \underline{r}\cdot(\underline{e}_{\underline{\iota}i}\times\underline{n})$ is constant for each side whose directional vector $\underline{e}_{\underline{\iota}i} = d\underline{l}_{\underline{\iota}}/dl_{\underline{\iota}}$ is chosen in a counterclockwise direction as the convention of the contour integral. The vertices composed of the

panel and the sides are also defined in a counterclockwise order. The field point is at an arbirary position except the side lines.

It is seen that the integral term for each side is related to the relative position of the field point with respect to the side. The integral, as will be shown, depends only on the coordinates of the two end points of the side.

In the self-induction case that the field point is just above or below the panel surface, since $\underline{n} \cdot \underline{r} = 0$ and then the second term in Eq. (7) vanishes, we get

$$\phi^{\prime\sigma} = -\frac{1}{4\pi} \underline{n} \cdot \oint_C \frac{\underline{r}}{r} \times d\underline{l}_\xi \qquad (11)$$

Equation (11) is reduced to, just setting $a = 0$ in Eq. (10)

$$\phi^{\prime\sigma} = -\frac{1}{4\pi} \sum_{i=1}^{N_s} b_i \int_{C_i} \frac{1}{r} dl_\xi \qquad (12)$$

Equation (12) is also valid for the case that the field point is on the outside extension plane of the planar panel.

Next, the corresponding velocity at the filed point is expressed as, in terms of only the first two integrals in Eq. (3),

$$\underline{V}^{\prime\sigma} = -\frac{1}{4\pi} \{ \underline{n} \oint_C \underline{A} \cdot d\underline{l}_\xi + \underline{n} \times \oint_C \frac{1}{r} d\underline{l}_\xi \} \qquad (13)$$

Rearrange this equation to yield

$$\underline{V}^{\prime\sigma} = -\frac{1}{4\pi} \{ \underline{n} \oint_C \frac{\underline{e} \times \underline{r}}{r(r+\underline{e} \cdot \underline{r})} \cdot d\underline{l}_\xi + \underline{n} \times \oint_C \frac{1}{r} d\underline{l}_\xi \}$$

$$= -\frac{1}{4\pi} \{ \underline{n}(\underline{n} \cdot \underline{e}) \sum_{i=1}^{N_s} b_i \int_{C_i} \frac{1}{r(r+a)} dl_\xi$$

$$+ \sum_{i=1}^{N_s} \underline{e}_{mi} \int_{C_i} \frac{1}{r} dl_\xi \}. \qquad (14)$$

where $\underline{e}_{mi} = \underline{n} \times \underline{e}_{li}$ (and then the unit vectors $\underline{n}$, $\underline{e}_{li}$ and $\underline{e}_{mi}$ are orthogonal each other).

Now we consider the self-induction case that the field point is just above the panel surface. The first integral in Eq. (13), which is evidently related to the solid angle subtended at the field point by the panel (see Eq. (6)), can be written as

$$\oint_C \underline{A} \cdot d\underline{l}_\xi = -\iint_S \underline{n} \cdot \nabla_\xi (\frac{1}{r}) dS_\xi = -2\pi. \qquad (15)$$

It can be derived by taking $\underline{e} = -\underline{n}$ (representing the approach of the field point toward the upper surface) and $\underline{e} \cdot \underline{r} = 0$ directly. Then Eq. (14) leads to

$$\underline{V}^{\prime\sigma} = \frac{1}{2} \underline{n} - \frac{1}{4\pi} \sum_{i=1}^{N_s} \underline{e}_{mi} \int_{C_i} \frac{1}{r} dl_\xi \qquad (16)$$

On the other hand, when x_p approaches toward the lower surface of the panel, the integral in Eq. (15) becomes 2π and then the sign of the first term in Eq. (16) is opposite. If x_p is on the (outside) extension plane of the planar panel, the first term in Eq. (16) vanishes. In this case, there is only the contribution from the second term in Eq. (13) associated with the geometrical skewness of the panel. If we take a field point at the centroid of a rectangular panel, the second term becomes zero since the contribution from one side (say, defined in $i = 1$) is canceled by that from the opposite side (defined in $i = 4$).

3. Constant Doublet Distribution

The potential at a field point x_p (x, y, z) induced by a doublet distribution of unit density $\mu = 1$ (recall that μ is defined as $\mu = -\phi$) over a planar panel is given by, taking only the first term from Eq. (4),

$$\phi^{(\mu)} = +\frac{1}{4\pi} \oint_c \underline{A} \cdot d\underline{l}_\zeta \tag{17}$$

Following the same manner as Eqs. (7) and (13), after some arrangement for $\underline{A}$ given in Eq. (6), we can write Eq. (17) as

$$\phi^{(\mu)} = +\frac{1}{4\pi} \oint_c \frac{\underline{e} \times \underline{r}}{r(r + \underline{e} \cdot \underline{r})} \cdot d\underline{l}_\zeta$$

$$= +\frac{1}{4\pi} (\underline{n} \cdot \underline{e}) \sum_{i=1}^{N_s} b_i \int_{C_i} \frac{1}{r(r+a)} d\underline{l}_\zeta \tag{18}$$

In the self-induction case that the field point is just above the panel, from Eq. (15) for $\oint_c \underline{A} \cdot d\underline{l}_\zeta$ it follows that

$$\phi^{(\mu)} = -\frac{\mu}{2} \tag{19}$$

It presents the correct behavior of the potential when a field point approaches the panel surface. For the case that the field point is on the (outside) extension of the planar panel, this expression is replaced by $\phi^{(\mu)} = 0$.

Now the corresponding induced velocity can be expressed by the line integral taken from Eq. (5)

$$\underline{V}^{(\mu)} = -\frac{1}{4\pi} \oint_c \nabla_\zeta (\frac{1}{r}) \times d\underline{l}_\zeta \tag{20}$$

Indeed the planarity assumption is not required for constant doublet strength distributions. Rewritiong this equation gives

$$\underline{V}^{(\mu)} = +\frac{1}{4\pi} \sum_{i=1}^{N_s} \underline{d}_i \int_{C_i} \frac{1}{r^3} d\underline{l}_\zeta \tag{21}$$

where $\underline{d}_i = \underline{r} \times \underline{e}_{li}$. Equation (20) has been often used in the lifting line theory and the lifting surface theory where a discrete vortex lattice may equivaletly be replaced by the uniform doublet distribution of the same vortex strength over the surface enclosed by the lattice. Unlike the potential, the

velocity has the continuous behavior (no-jump) when the field point crosses the panel surface.

4. Closed-Forms of the Basic Integrals

In the preceding sections, we have expressed the induced potentials and velocities in forms of a sum of the more simplified line integral given in Eqs. (10), (14), (18), (21). Since these equations cover inherently the self-induction cases (see Eqs. (12), (16), (19)), we will derive here closed-forms of the following line integrals (of four types) involved in Eqs. (10), (14), (18), (21) :

$$I1_i = \int_{C_i} \frac{1}{r} d\underline{l}_\zeta, \qquad I2_i = \int_{C_i} \frac{1}{r+a} d\underline{l}_\zeta,$$

$$I3_i = \int_{C_i} \frac{1}{r(r+a)} d\underline{l}_\zeta, \qquad I4_i = \int_{C_i} \frac{1}{r^3} d\underline{l}_\zeta$$

The line integrals for each side of the polygon can be treated independently by the geometric parameters of that side. It is sufficient, therefore, to consider only one side of the panel, say $i = 1$, for the purpose of these evaluations. For simplicity of the presentation, we drop the subscript i used for identifying the side. We take, without loss of generality, a local plane coordinate system (x', z') in the plane through the field point x_p and the side concerned, such that the side lies on the x'-axis, one end point of the side is at the origin and the integration path is performed along the positive x'-axis, as shown in Fig. 1.

The reason that we have chosen the local coordinate system is that, as will be shown, the final closed-forms of the basic integrals would be much more compact than those expressed in the global coordinate system, even although both forms can produce identical results.

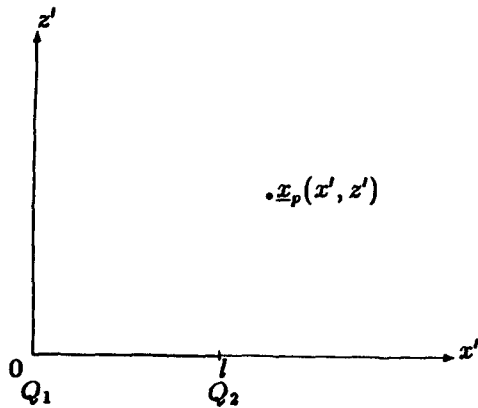The end points of the side of length l are expres-

Fig. 1 : A local plane coordinate

sed in two coordinate systems, namely, by Q_1 $(x_1,$ $y_1, z_1)$ and Q_2 (x_2, y_2, z_2) in the global coordinate system, and by Q_1 $(0, 0)$ and Q_2 $(l, 0)$ in the local plane coordinate system. The field point is also defined by x_p (x_p, y_p, z_p) and x_p (x', z') respectively. Then the local coordinates (x', z') can be expressed in terms of the global coordinates as follows :

The vectors $\overline{Q_1 Q_2}$ and $\overline{Q_1 x_p}$ are written as, in the global coordinate system,

$$\overline{Q_1 Q_2} = (x_2 - x_1) i + (y_2 - y_1) i + (z_2 - z_1) k$$
$$\overline{Q_1 x_p} = (x_p - x_1) i + (y_p - y_1) i + (z_p - z_1) k$$

Applying the relation for the magnitude of the cross product of the two vectors $| \overline{Q_1 Q_2} \times \overline{Q_1 x_p} | = | \overline{Q_1 Q_2} | | z' |$, we get $| z' | = | e_i \times \overline{Q_1 x_p} |$. From the dot product of the two vectors $\overline{Q_1 Q_2} \cdot \overline{Q_1 x_p} = | \overline{Q_1 Q_2} | x'$, it follows that $x' = e_i \cdot \overline{Q_1 x_p}$.

To simply the notation in hte following development, we drop the prime($'$) in x' and z' and define the distances between the end points and the field point by $R_1 \equiv | \overline{Q_1 x_p} | = \sqrt{x^2 + z^2}$ and $R_2 \equiv | \overline{Q_2} x_p | = \sqrt{(l-x)^2 + z^2}$. The integegral forms given by Gradshteyn & Ryzhik (1965) (on pages 68, 81, 84) have been used.

(1) For the integral $I1 = \int_c \frac{1}{r} dl_\xi$, expressing

the integral in terms of the local coordinates x and z and introducing an integration variable ξ, we get

$$I1 = \int_0^l \frac{1}{\sqrt{(x-\xi)^2 + z^2}} d\xi$$
$$= \ln \frac{R_2 + l - x}{R_1 - x} \quad (\text{or } \ln \frac{R_1 + x}{R_1 - (l - x)})$$

This expressions is also valid for the cases of $z = 0$, that is, of that the field point is on the extension line of the side.

(2) The evaluation of the integral $I2 = \int_c \frac{1}{r+a} dl_\xi$, requires more complicated algebraic manipulation and only the final results with a brief description are presented here. First we transform the integration variable ξ into

$t = \sqrt{(x - \xi)^2 + z^2 + a}$ for use of an integrable form. Then two cases depending on the value of x should be considered as follows :

(i) When $x \leq 0$ or $x \geq l$, we get, after some arrangement with the new integration limits $L = R_1 + a$ and $U = R_2 + a$,

$$I2 = \int_L^U \frac{t - a}{t \sqrt{t^2 - 2at + a^2 - z^2}} dt$$
$$= I1 - \frac{a}{\sqrt{z^2 - a^2}} \sin^{-1}(H) \quad (22)$$

where

$$H = \frac{\sqrt{z^2 - a^2} \{z^2 l + a(l-x) R_1 + axR_2\}}{z^2 (R_1 + a)(R_2 + a)}$$

or $\frac{l \sqrt{z^2 - a^2}}{z_2 (R_1 + a)(R_2 + a)} \{1 + \frac{a(l - 2x)}{(l-x) R_1 - xR_2}\}$

Here for efficient computation, we have used the trigonometric addition formulae to combine the pair of arcsine functions appeared in the manipulation.

(ii) When $0 < x < l$, the integration interval $[0, l]$ is divided into two parts $[0, x]$ and $[x, l]$ to which the previous procedure can

be applied separately.

$$I2 = (\int_0^x + \int_x^l) \frac{1}{\sqrt{(x-\xi)^2 + z^2} + a} \, d\xi$$

$$= I1 - \frac{a}{\sqrt{z^2 - a^2}} \{\pi - \sin^{-1}(H)\} \quad (23)$$

Equation (23) is valid if the following restriction that appears in the use of the trigonometric addition formulae (Gradshteyn & Ryzhik, p. 48) holds, otherwise we take Eq. (22) :

$$(R_1 + a)^2 (z^2 + aR_2)^2$$

$$+ (R_2 + a)^2 (z^2 + aR_1)^2$$

$$\leq z^2 (R_1 + a)^2 (R_2 + a)^2$$

If $z^2 = a^2$, the integral I2 becomes the more simplified form :

$$I2 = I1 - (\frac{x}{R_1 + a} + \frac{l-x}{R_2 + a})$$

(3) For the integral $I3 = \int_c \frac{1}{r(r+a)} dl_\xi$, we take a partial fraction for the integrand (unless $a = 0$) and directly use the results in the cases (1) and (2) :

$$I3 = \frac{1}{a}\int_0^l (\frac{1}{r} - \frac{1}{r+a}) \, d\xi = \frac{1}{a}(I_1 - I_2)$$

But if $a = 0$, a direct integration yields

$$I3 = \int_0^l \frac{1}{(x-\xi)^2 + z^2} d\xi$$

$$= \frac{1}{|z|} (\arctan \frac{l-x}{|z|} + \arctan \frac{x}{|z|})$$

Furthermore if $a = 0$ and $z = 0$, then

$$I3 = \int_0^l \frac{1}{(x-\xi)^2} \, d\xi = \frac{l}{x(x-l)}$$

(4) The integral $I4 = \int_c \frac{1}{r^3} dl_\xi$, can also be performed directly, yielding

$$I4 = \int_0^l \frac{1}{\sqrt{(x-\xi)^2 + z^2}^3} \, d\xi$$

$$= \frac{1}{z^2} \{\frac{l-x}{R_2} + \frac{x}{R_1}\}$$

If $z = 0$, it is replaced by

$$I4 = \int_0^l \frac{1}{|x-\xi|^3} \, d\xi$$

$$= +\frac{1}{2} \{\frac{1}{(l-x)^2} - \frac{1}{x^2}\} \quad \text{for } x>l$$

$$-\frac{1}{2} \{\frac{1}{(l-x)^2} - \frac{1}{x^2}\} \quad \text{for } x>0$$

When the inverse trigonometric functions are implemented in the computational algorithm, their values may be evaluated in the inverval $[-\pi/2, \pi/2]$ without considering the separate arguments of the functions.

5. Extension to Linear Distributions

In this section the preceding analyses are extended to include a linear distribution of sources and doublets over a planar panel. In order to determine the distribution shape uniquely, it is enougt to take only three points (that are not collinear) of a polygon. We consider therefore a triangular panel of a linear source distribution herein (the following procedure can be applied similarly to the doublet distribution). A gradient form of the linear varying source strength distributed on the panel is specified as

$$\nabla \sigma = \alpha \underline{i} + \beta \underline{j} + \gamma \underline{k}$$

The coofficients α, β and γ are determined from the singularity strength values at the vertices, by using the fact that the vector $\nabla \sigma$ is parallel to the panel. Define the source strengths at the vertices by σ_i, ($i = 1, 2, 3$) and the vertex positions by (x_i,

y_i, z_i). Then we can form a linear equation system for α, β and γ :

$$\nabla \sigma \cdot \underline{e}_{li} \equiv \frac{\sigma_{i+1} - \sigma_i}{l_i}$$

$$= \frac{\alpha\,(x_{i+1} - x_i) + \beta\,(y_{i+1} - y_i) + \gamma\,(z_{i+1} - z_i)}{l_i}$$

$$(i = 1, 2, 3)$$

Here recall that the vertices and the sides are defined in a counterclockwise sense and the index 4 corresponds to 1 by the cyclic convention. By the Cramer's rule, α, β and γ are determined :

$$\alpha = \det\,(\sigma_i - \sigma_{i+1},\ y_i - y_{i+1},\ z_i - z_{i+1})/\triangle$$

$$\beta = \det\,(x_i - x_{i+1},\ \sigma_i - \sigma_{i+1},\ z_i - z_{i+1})/\triangle$$

$$\gamma = \det\,(x_i - x_{i+1},\ y_i - y_{i+1},\ \sigma_i - \sigma_{i+1})/\triangle$$

where $\det(\cdots)$ denotes the determinant of a matrix and $\triangle = \det(x_i - x_{i+1}, y_i - y_{i+1}, \sigma_i - \sigma_{i+1})$. Now in order to derive closed-forms for Eqs.(2) through (5) including the linear variation terms, we introduce first the following basic integrals to be evaluated additionally :

$$J1_i = \int_{C_i} \frac{\xi}{r}\,d\xi, \qquad J2_i = \int_{C_i} \frac{\xi}{r+a}\,d\xi,$$

$$J3_i = \int_{C_i} \frac{\xi}{r(r+a)}\,d\xi, \qquad J4_i = \int_{C_i} \frac{\xi}{r^3}\,d\xi,$$

$$J5_i = \int_{C_i} r\,d\xi, \qquad J6_i = \int_{C_i} \ln(r+a)\,d\xi$$

Since we can superpose the contribution of the associated line integrals for each side like the constant distribution cases, we drop the subscript i for simple notation. The evaluation of these integrals is considerably straightforward and only the final results are presented here, without explicit manipulation, with using the basic integrals obatined in the previous section :

$$J1 = R_2 - R_1 + xI1$$

$$J2 = R_2 - R_1 - a\ln\frac{R_2 + a}{R_1 + a} + xI2$$

$$J3 = \ln\frac{R_2 + a}{R_1 + a} + xI3$$

$$J4 = \frac{1}{R_1} - \frac{1}{R_2} + xI4$$

$$J5 = \frac{1}{2}\,\{(l-x)R_2 + xR_1 + z^2\,I1\}$$

$$J6 = (1-x)\ln(R_2 + a) + x\ln(R_1 + a) - l + aI1$$
$$\qquad + (z^2 - a^2)\,I3$$

The closed-forms of Eqs.(2) through (5) for the potentials and velocities due to the linear distributions can be expressed in terms of the basic integrals in a form analogous to those of the constant distibutions, after recovering the index i for the side and vertex :

$$\phi^{(\sigma)} = -\frac{1}{4\pi}\sum_{i=1}^{N_s} b_i\,(\sigma_i\,I2_i + \nabla\sigma \cdot \underline{e}_{li}\ J2_i)$$
$$\qquad + \nabla\sigma \cdot \underline{e}_{mi}\,(J6_i - aJ5_i) \tag{24}$$

$$\underline{V}^{(\sigma)} = -\frac{1}{4\pi}\sum_{i=1}^{N_s} [\underline{n}(\underline{n}\cdot\underline{e})\,\{b_i\,(\sigma_i\,I3_i + \nabla\sigma \cdot \underline{e}_{li}\,J3_i)$$
$$\qquad + \nabla\sigma \cdot \underline{e}_{mi}\,J6_i\} + \underline{e}_{mi}\,(\sigma_i\,I1_i + \nabla\sigma \cdot \underline{e}_{li}\,J1_i)$$
$$\qquad + \nabla\sigma\,b_i\,I2_i] \tag{25}$$

$$\phi^{(\mu)} = +\frac{1}{4\pi}(\underline{n}\cdot\underline{e})\sum_{i=1}^{N_s}\{b_i\,(\mu_i\,I3_i + \nabla\mu \cdot \underline{e}_{li}\,J3_i)$$
$$\qquad + \nabla\mu \cdot \underline{e}_{mi}\,J6_i\} \tag{26}$$

$$\underline{V}^{(\mu)} = +\frac{1}{4\pi}\sum_{i=1}^{N_s}\{d_i\,(\mu_i\,I4_i + \nabla\mu \cdot \underline{e}_{li}\,J4_i)$$
$$\qquad + \nabla\mu\,(\underline{n}\cdot\underline{e})\,b_i\,I3_i - \underline{n}\,\nabla\mu \cdot \underline{e}_{mi}\,I1_i\} \tag{27}$$

Neglecting the terms involving $\nabla\sigma$, we can of course reduce these expressions to the results for the case of constant singularity distributions derived already in the preceding sections. It confirms easily that the normal component of $\underline{V}^{(\sigma)}$ has the same form as $\phi^{(\mu)}$ except notation of the singularity.

6. Test Calculations for Constant Distributions

The present analysis was programmed for practical implementation (Suh (1990b)) and was verified by comparing the induced potedtials and velocities obtained by the present method with those by the method of Newman. The comparison was based on the computer output for several cases of the constant singularity distributions. It was found that the resultant values are same up to the significant figures allowed by truncation or round-off error of a computer (but the details are not presented here). Thus only in the following extreme cases, comparison of analytic integration with numerical integration is provided herein to check a sensitivity of the calculation. A planar rectangular element of 12×1 (i.e., aspect ratio is 12) is taken for the test

calculations. It may be assumed that the element is in the plane $z = 0$ with the four vertices at (0,0,0), (1,0,0), (1,12,0), (0,12,0), respectively. We take various field points in the extreme vicinity of the element surface or one vertes. Their coordinates are, with alphabetical labelling, A (0.5,6.0,+0.0), B (0.5,6.0,+0.00001), C (0.5,6.0,−0.00001), D (0.0,−0.00001, 0.0), E (0.0,0.0,+0.00001), F (0.0,0.0,−0.00001). The points A, B and C are, respectively, on, just above and below of the centroid of the element and D, E and F are very near the origin. The constant densities of cource and doublet distributions are taken with 1, (i.e., $\sigma = 1$, $\mu = 1$).

First we will compare numerical integrations and analytical evaluations of the basic integrals described in section 4. At the field points A, D and F, the values of the integrals for each side are compared in Tables 1,2 and 3, respectively. With and Apo-

Table 1. Comparison of the basic integrals by analytic and numerical calculation at point A (0.5, 6.0, +0.0)

	Side	Gaussian-Quadrature Points, $N =$				Analytic
		20	100	500	2500	
$\int \dfrac{1}{r} d\xi$	1	.1665E+00	.1665E+00	.1665E+00	.1665E+00	.1665E+00
	2	.6275E+01	.6360E+01	.6360E+01	.6360E+01	.6360E+01
	3	.1665E+00	.1665E+00	.1665E+00	.1665E+00	.1665E+00
	4	.6275E+01	.6360E+01	.6360E+01	.6360E+01	.6360E+01
$\int \dfrac{1}{(r+a)} d\xi$	1	.1665E+00	.1665E+00	.1665E+00	.1665E+00	.1665E+00
	2	.6275E+01	.6360E+01	.6360E+01	.6360E+01	.6360E+01
	3	.1665E+00	.1665E+00	.1665E+00	.1665E+00	.1665E+00
	4	.6275E+01	.6360E+01	.6360E+01	.6360E+01	.6360E+01
$\int \dfrac{1}{r(r+a)} d\xi$	1	.2771E−01	.2771E−01	.2771E−01	.2771E−01	.2771E−01
	2	.5550E+01	.5951E+01	.5951E+01	.5951E+01	.5951E+01
	3	.2771E−01	.2771E−01	.2771E−01	.2771E−01	.2771E−01
	4	.5550E+01	.5951E+01	.5951E+01	.5951E+01	.5951E+01
$\int \dfrac{1}{r^3} d\xi$	1	.4614E−02	.4614E−02	.4614E−02	.4614E−02	.4614E−02
	2	.6688E+01	.7972E+01	.7972E+01	.7972E+01	.7972E+01
	3	.4614E−02	.4614E−02	.4614E−02	.4614E−02	.4614E−02
	4	.6688E+01	.7972E+01	.7972E+01	.7972E+01	.7972E+01

Table 2. Comparison of the basic integrals by analytic and numerical calculation at point D
(0.0, -0.00001, 0.0)

	Side	Gaussian-Quadrature Points, $N =$				Analytic
		20	100	500	2500	
$\int \dfrac{1}{r} d\xi$	1	.7195E+01	.1037E+02	.1224E+02	.1221E+02	.1221E+02
	2	.3180E+01	.3180E+01	.3180E+01	.3180E+01	.3180E+01
	3	.8324E-01	.8324E-01	.8324E-01	.8324E-01	.8324E-01
	4	.7195E+01	.1036E+02	.1322E+02	.1400E+02	.1400E+02
$\int \dfrac{1}{(r+a)} d\xi$	1	.7195E+01	.1037E+02	.1224E+02	.1221E+02	.1221E+02
	2	.3180E+01	.3180E+01	.3180E+01	.3180E+01	.3180E+01
	3	.8324E-01	.8324E-01	.8324E-01	.8324E-01	.8324E-01
	4	.7195E+01	.1036E+02	.1322E+02	.1400E+02	.1400E+02
$\int \dfrac{1}{r(r+a)} d\xi$	1	.8400E+03	.2011E+05	.1636E+06	.1571E+06	.1571E+06
	2	.1488E+01	.1488E+01	.1488E+01	.1488E+01	.1488E+01
	3	.6928E-02	.6928E-02	.6928E-02	.6928E-02	.6928E-02
	4	.6997E+02	.1666E+04	.3280E+05	.9971E+05	.1000E+06
$\int \dfrac{1}{r^3} d\xi$	1	.2211E+06	.1266E+09	.1084E+11	.1000E+11	.1000E+11
	2	.9965E+00	.9965E+00	.9965E+00	.9965E+00	.9965E+00
	3	.5767E-03	.5767E-03	.5767E-03	.5767E-03	.5767E-03
	4	.1535E+04	.8705E+06	.3660E+09	.4927E+10	.5000E+10

llo Workstation DN 10000, high precision was used in Fortran program. The influences of the basic integrals at the field points by the respective sides of the element are listed. In the tables, the side 1 denotes the line between the vertices (0,0,0) and (1,0,0) and the other sides are numbered in counterclockwise order in a similar way. In the numerical calculations, the Gaussian quadratures with various quadrature-base points were used to show convergence of numerical integration. Some loss in accuracy of numerical integrations appears when the field point is very close from the sides or the vertices, and its amount depends on the number of the quadrature-base points used.

As expected, the difference between the analytical results and the numerical results increases with the order of r in the denominator of the integrand, and decreases with the distance of a field point from the sides (or vertices). It is seen that for a field point having a numerically singular behavior in the line integral, many quadrature-base points, even up to 2500, is required to reach the same order as the analytical evalutions. It implies that a numerical integration results in a large amount of computer time undesirably.

The induced velocities and potentials at the selected field points are compared in Tables 4 through 9 in the same fashion in order to confirm the aforementioned advantages in computation efficiency. In Tables 4,5 and 6, it is observed that the analytic integration gives the correct singular behavior as the field point approach the centroid of the panel.

Table 3. Comparison of the basic integrals by analytic and numerical calculation at point E
(0.0, 0.0, +0.00001)

	Side	Gaussian-Quadrature Points, $N =$				Analytic
		20	100	500	2500	
$\int \dfrac{1}{r}\,d\xi$	1	.7195E+01	.1037E+02	.1224E+02	.1221E+02	.1221E+02
	2	.3180E+01	.3180E+01	.3180E+01	.3180E+01	.3180E+01
	3	.8324E−01	.8324E−01	.8324E−01	.8324E−01	.8324E−01
	4	.7195E+01	.1037E+02	.1356E+02	.1469E+02	.1469E+02
$\int \dfrac{1}{(r+a)}\,d\xi$	1	.7187E+01	.1018E+02	.1121E+02	.1121E+02	.1121E+02
	2	.3180E+01	.3180E+01	.3180E+01	.3180E+01	.3180E+01
	3	.8324E−01	.8324E−01	.8324E−01	.8324E−01	.8324E−01
	4	.7195E+01	.1036E+02	.1320E+02	.1369E+02	.1369E+02
$\int \dfrac{1}{r(r+a)}\,d\xi$	1	.8378E+03	.1893E+05	.1025E+06	.1000E+06	.1000E+06
	2	.1488E+01	.1488E+01	.1488E+01	.1488E+01	.1488E+01
	3	.6928E−02	.6928E−02	.6928E−02	.6928E−02	.6928E−02
	4	.6998E+02	.1674E+04	.3636E+05	.9987E+05	.1000E+06
$\int \dfrac{1}{r^3}\,d\xi$	1	.2211E+06	.1266E+09	.1084E+11	.1000E+11	.1000E+11
	2	.9965E+00	.9965E+00	.9965E+00	.9965E+00	.9965E+00
	3	.5767E−03	.5767E−03	.5767E−03	.5767E−03	.5767E−03
	4	.1536E+04	.8856E+06	.5284E+09	.1004E+11	.1000E+11

Table 4. Comparison of potentials and velocities by analytic and numerical calculation at point A
(0.5, 6.0, +0.0)

	Gaussian-Quadrature Points, $N =$				Analytic
	20	100	500	2500	
$\phi^{(\sigma)}$	-0.6583E+00	-0.6650E+00	-0.6650E+00	-0.6650E+00	-0.6650E+00
$V_x^{(\sigma)}$	0.0000E+00	0.0000E+00	0.0000E+00	0.0000E+00	0.0000E+00
$V_y^{(\sigma)}$	0.0000E+00	0.0000E+00	0.0000E+00	0.0000E+00	0.0000E+00
$V_z^{(\sigma)}$	0.4681E+00	0.5000E+00	0.5000E+00	0.5000E+00	0.5000E+00
$\phi^{(\mu)}$	-0.4681E+00	-0.5000E+00	-0.5000E+00	-0.5000E+00	-0.5000E+00
$V_x^{(\mu)}$	0.0000E+00	0.0000E+00	0.0000E+00	0.0000E+00	0.0000E+00
$V_y^{(\mu)}$	0.0000E+00	0.0000E+00	0.0000E+00	0.0000E+00	0.0000E+00
$V_z^{(\mu)}$	0.5366E+00	0.6388E+00	0.6388E+00	0.6388E+00	0.6388E+00

It is found that the values of $V_z^{(\sigma)}$, $\phi^{(\mu)}$, $\phi^{(\sigma)}$, and $V_z^{(\mu)}$ obtained by the numerical integration with 20 quadrature points ($N = 20$) are inaccurated compared with those obtained with more number of the quadrature points. These features are profound when the field points are near the vertex as shown

Table 5. Comparison of potentials and velocities by analytic and numerical calculation at point B
(0.5, 6.0, +0.00001)

	Gaussian-Quadrature Points, $N =$				Analytic
	20	100	500	2500	
$\phi^{(o)}$	-0.6583E+00	-0.6650E+00	-0.6650E+00	-0.6650E+00	-0.6650E+00
$V_x^{(o)}$	0.0000E+00	0.0000E+00	0.0000E+00	0.0000E+00	0.0000E+00
$V_y^{(o)}$	0.0000E+00	0.0000E+00	0.0000E+00	0.0000E+00	0.0000E+00
$V_z^{(o)}$	0.4681E+00	0.5000E+00	0.5000E+00	0.5000E+00	0.5000E+00
$\phi^{(\mu)}$	-0.4681E+00	-0.5000E+00	-0.5000E+00	-0.5000E+00	-0.5000E+00
$V_x^{(\mu)}$	0.5371E-21	0.2791E-22	0.5166E-21	0.3339E-21	0.2264E-21
$V_y^{(\mu)}$	-0.5143E-25	0.2006E-00	0.2288E-25	0.2600E-24	0.2309E-24
$V_z^{(\mu)}$	0.5366E+00	0.6388E+00	0.6388E+00	0.6388E+00	0.6388E+00

Table 6. Comparison of potentials and velocities by analytic and numerical calculation at point C
(0.5, 6.0, -0.00001)

	Gaussian-Quadrature Points, $N =$				Analytic
	20	100	500	2500	
$\phi^{(o)}$	-0.6583E+00	-0.6650E+00	-0.6650E+00	-0.6650E+00	-0.6650E+00
$V_x^{(o)}$	0.0000E+00	0.0000E+00	0.0000E+00	0.0000E+00	0.0000E+00
$V_y^{(o)}$	0.0000E+00	0.0000E+00	0.0000E+00	0.0000E+00	0.0000E+00
$V_z^{(o)}$	-0.4681E+00	-0.5000E+00	-0.5000E+00	-0.5000E+00	-0.5000E+00
$\phi^{(\mu)}$	0.4681E+00	0.5000E+00	0.5000E+00	0.5000E+00	0.5000E+00
$V_x^{(\mu)}$	-0.5371E-21	-0.2791E-22	-0.5166E-21	-0.3339E-21	-0.2264E-21
$V_y^{(\mu)}$	0.5143E-25	-0.2006E-25	-0.2288E-25	-0.2600E-24	-0.2309E-24
$V_z^{(\mu)}$	0.5366E+00	0.6388E+00	0.6388E+00	0.6388E+00	0.6388E+00

Table 7. Comparison of potentials and velocities by analytic and numerical calculation at point D
(0.0, -0.00001, 0.0)

	Gaussian-Quadrature Points, $N =$				Analytic
	20	100	500	2500	
$\phi^{(o)}$	-0.3325E+00	-0.3325E+00	-0.3325E+00	-0.3325E+00	-0.3325E+00
$V_x^{(o)}$	-0.3195E+00	-0.5712E+00	-0.7986E+00	-0.8608E+00	-0.8609E+00
$V_y^{(o)}$	-0.5660E+00	-0.8185E+00	-0.9672E+00	-0.9647E+00	-0.9647E+00
$V_z^{(o)}$	0.1243E+00	0.1090E+00	-0.5212E-02	-0.2325E-10	0.4199E-17
$\phi^{(\mu)}$	-0.1243E+00	-0.1090E+00	0.5212E-02	0.2325E-10	-0.4199E-17
$V_x^{(\mu)}$	0.0000E+00	0.0000E+00	0.0000E+00	0.0000E+00	0.0000E+00
$V_y^{(\mu)}$	0.0000E+00	0.0000E+00	0.0000E+00	0.0000E+00	0.0000E+00
$V_z^{(\mu)}$	-0.9611E-01	-0.1007E+03	-0.8628E+04	-0.7958E+04	-0.7958E+04

Table 8.　Comparison of potentials and velocities by analytic and numerical calculation at point E
(0.0, 0.0, -0.00001)

		Gaussian-Quadrature Points, $N =$				Analytic
		20	100	500	2500	
$\phi^{(\sigma)}$		-0.3325E+00	-0.3325E+00	-0.3325E+00	-0.3325E+00	-0.3325E+00
$V_x^{(\sigma)}$		-0.3196E+00	-0.5726E+00	-0.8259E+00	-0.9159E+00	-0.9160E+00
$V_y^{(\sigma)}$		-0.5660E+00	-0.8185E+00	-0.9672E+00	-0.9647E+00	-0.9647E+00
$V_z^{(\sigma)}$		0.1250E+00	0.1250E+00	0.1250E+00	0.1250E+00	0.1250E+00
$\phi^{(\mu)}$		-0.1250E+00	-0.1250E+00	-0.1250E+00	-0.1250E+00	-0.1250E+00
$V_x^{(\mu)}$		-0.1221E-02	-0.7047E+00	-0.4205E+03	-0.7987E+04	-0.7958E+04
$V_y^{(\mu)}$		-0.1760E+00	-0.1008E+03	-0.8628E+04	-0.7958E+04	-0.7958E+04
$V_z^{(\mu)}$		0.7985E-01	0.7985E-01	0.7985E-01	0.7985E-01	0.7985E-01

Table 9.　Comparison of potentials and velocities by analytic and numerical calculation at point F
(0.0, 0.0, -0.00001)

		Gaussian-Quadrature Points, $N =$				Analytic
		20	100	500	2500	
$\phi^{(\sigma)}$		-0.3325E+00 .	-0.3325E+00	-0.3325E+00	-0.3325E+00	-0.3325E+00
$V_x^{(\sigma)}$		-0.3196E+00	-0.5726E+00	-0.8259E+00	-0.9159E+00	-0.9160E+00
$V_y^{(\sigma)}$		-0.5660E+00	-0.8185E+00	-0.9672E+00	-0.9647E+00	-0.9647E+00
$V_z^{(\sigma)}$		-0.1250E+00	-0.1250E+00	-0.1250E+00	-0.1250E+00	-0.1250E+00
$\phi^{(\mu)}$		0.1250E+00	0.1250E+00	0.1250E-00	0.1250E+00	0.1250E+00
$V_x^{(\mu)}$		0.1221E-02	0.7047E+00	0.4205E+03	0.7987E+04	0.7958E+04
$V_y^{(\mu)}$		0.1760E+00	0.1008+03	0.8628E+04	0.7958E+04	0.7958E+04
$V_z^{(\mu)}$		0.7985E-01	0.7985E-01	0.7985E-01	0.7985E-01	0.7985E-01

in Tables 7,8 and 9 and appear even for the cases of the other quadrature points. Much more number of the quadrature points are required to achieve considerably accurate values.

7. Concluding Remarks

The closed-forms (Eqs. (24) through (27)) provided in section 5 (in particular for the induced velocities) are reatively much simpler than those given by Webster (1975) and are more explicit than those given by Newman (1986), although it is very diffi-

cult to show precisely the identities which exist among their expressions and the present ones because of the difference of the local coordinate systems used. These explicit simple expressions (even for the linear distributions) may reduce the computer time significantly for formation of a set of simultaneous linear equations. In the potential-based panel methods, for example, the calculated potentials form the fundamental matrix elements of the linear system to be soved and thus such a formation is the primary factor of the computer time. Also the present expressions may be used in complex-flow

problems(in some of which we should often put a careful effort for field points located inevitably in the extreme vicinity of the panel edges) to find accurately, for example, (i) a convection velocity of circulation values at the wake sheet of a lifting body, (ii) potential and velocity distributions at a hull surface induced by propellers in propeller-hull interaction problems, and and (iii) induced potential and velocity in mutual interaction problems such as ducted propellers and compound propellers.

We found the newly useful relation of Eq. (9) which can be applied directly to calculation of the volumetric integral of vorticity distributions given by the Biot-Savart integral. This integral would often require to be evaluated when the vorticity-velocity formulation is used in inviscid rotational flow problems involving shear-flow interaction. For piecewise constant vorticity distribution within a volumetric element with planar faces, we can first transform the volume integral the surface integrals on the enclosed faces by using Gauss theorem. The integrand of the transformed surface integrals becomes $1/r$ and then Eq. (9) (with $e = \pm n$) can be used to tiansform each surface integral into the line integrals expressed a form analogous to Eq.(8).

Acknowledgements

References

[1] Cantaloube, B. and Rehbach, C., "Calculdes Integrales de la Methode des Singularites," Recherche Aerospatiale, n° 1, pp. 15—22, 1986 "Calculation of the Integrals of the Singularity Method,"Aerospace Research, No. 1, pp.15—22

[2] Gradshteyn, I.S. and Ryzhik, I.M. *Table of Integrals, Series and Products*, Academic Press, *Inc., New York and London*, 1965

[3] Guiraud, J.P., "Potential of Velocities Generated by a Localized Vortex Distribution," Aerospace Research, English Translation-ESA-TT-560, 1978

[4] Hess, J.L. and Smith, A.M.O., "Calculation of Potential Flow about Arbitrary Bodies," Progress in Aeronautical Science Series, Pergamon Press, Vol. 8, 1966.

[5] Newman, J.N., "Distributions of Sources and Normal Dipoles over a Quadrilateral Panel," *Journal of Engineering Mathematics*, Vol. 20, 1986

[6] Suh, J.C., "Review of the Paper : Calculation of the Integrals of the Singularity Method by Cantaloube and Rehbach," KRISO Propulsor Technology Laboratory Report, No. 22—90, 1990a

[7] Suh, J.C., "Analytic Evaluations of the Induction-Integrals for Distributions of Sources and Doublets over a Planar Polygon Element," KRISO Propulsor Technology Laboratory Report, No. 23—90. 1990b

[8] Webster, W.C., "The Flow About Arbitrary, Three-Dimensional Smooth Bodies," *Journal of Ship Research*, Vol. 19. No. 4, 1975